

## Analysis of persistence during intracellular actin-based transport mediated by molecular motors

This content has been downloaded from IOPscience. Please scroll down to see the full text.

2010 J. Phys.: Conf. Ser. 246 012038

(<http://iopscience.iop.org/1742-6596/246/1/012038>)

View [the table of contents for this issue](#), or go to the [journal homepage](#) for more

Download details:

IP Address: 157.92.4.71

This content was downloaded on 04/06/2015 at 21:54

Please note that [terms and conditions apply](#).

# Analysis of persistence during intracellular actin-based transport mediated by molecular motors

C. Pallavicini<sup>1</sup>, M. A. Despósito<sup>1,3</sup>, V. Levi<sup>1,2,3</sup> and L. Bruno<sup>1,3</sup>

<sup>1</sup> Departamento de Física, Facultad de Ciencias Exactas y Naturales, Universidad de Buenos Aires, 1428 Buenos Aires, Argentina.

<sup>2</sup> Departamento de Química Biológica, Facultad de Ciencias Exactas y Naturales, Universidad de Buenos Aires, 1428 Buenos Aires, Argentina.

<sup>3</sup> Consejo Nacional de Investigaciones Científicas y Técnicas, Argentina.

E-mail: lbruno@df.uba.ar

## Abstract.

The displacement of particles or probes in the cell cytoplasm as a function of time is characterized by different anomalous diffusion regimes. The transport of large cargoes, such as organelles, vesicles or large proteins, involves the action of ATP-consuming molecular motors. We investigate the motion of pigment organelles driven by myosin-V motors in *Xenopus laevis* melanocytes using a high spatio-temporal resolution tracking technique. By analyzing the turning angles ( $\phi$ ) of the obtained 2D trajectories as a function of the time lag, we determine the critical time of the transition between anticorrelated and directed motion as the time when the turning angles begin to concentrate around  $\phi = 0$ . We relate this transition with the crossover from subdiffusive to superdiffusive behavior observed in a previous work [5]. We also assayed the properties of the trajectories in cells with inhibited myosin activity, and we can compare the results in the presence and absence of active motors.

## 1. Introduction

Our knowledge of intracellular transport of organelles mediated by molecular motors has markedly increased thanks to the improvement of single particle tracking (SPT) techniques. In STP experiments a probe particle or organelle is followed and tracked with millisecond temporal resolution and nanometer precision (see e.g. [1]). In this way, 2D trajectories of the motion of the particles are recovered.

Traditionally, two-dimensional trajectories are characterized by studying the statistical behavior of the mean square displacement (MSD) as a function of the time lag  $\tau$ . The MSD measures the mean square distance between two points belonging to the trajectory and separated by a time lapse  $\tau$ .

Although the MSD is a useful magnitude that has been used to determine the different diffusive regimes of intracellular particles motion (see e.g. [2, 3, 4, 5]), it hides relevant information about the direction or persistence of the motion. For example, in [6, 7] the cytoskeleton remodeling dynamics is studied by analyzing the motion of microbeads bound to the cytoskeleton filaments. In that system, the MSD of the microbeads undergoes a transition from subdiffusive to superdiffusive behavior with time. However, the authors were able to provide evidence of the processes that regulate the dynamics -i.e. caged dynamics at short time scales

and directional memory at long time lags- only when they based their analysis on the turning angles distribution properties. Even though it is well known that molecular motors are proteins able to convert the energy form adenosine triphosphate (ATP) hydrolysis into directed motion along cytoskeleton filaments, the persistence of motor-driven cargoes motion in intracellular transport remains unclear.

Interestingly, recent theoretical works have been devoted to the origin of the competition between sub- and superdiffusive transport in different physical models [8, 9, 10]. *Xenopus laevis* melanophores are a unique system where motor-driven transport can be studied since they have pigment organelles or melanosomes containing the black pigment melanin, therefore they can be followed using bright-field transmission light microscopy [11]. Three different classes of motors are responsible for pigment organelles transport in *Xenopus laevis* melanophores cells: kinesin II and dynein move cargoes along microtubules and myosin-V carries them along actin filaments [12, 13, 14].

In a very recent paper, we study the different anomalous regimes of myosin-V driven melanosomes in cells treated with nocodazole, a drug that depolymerizes microtubules [5]. There we reported a transition from a subdiffusive to a superdiffusive regime based on the behavior of the MSD over time, computed from the 2D trajectories obtained by SPT.

In this work, we go further with the analysis of myosin-V driven melanosomes: we compute the turning angle distributions from the 2D trajectories. Using this approach, we were able to correlate the transition from sub- to superdiffusive behavior with the antipersistent-persistent change in the turning angles distributions. We compare the results in the presence and absence of active motors with the aid of parallel experiments performed in mutant cells with inhibited myosin-V activity.

## 2. Turning angles

We analyzed trajectories of melanosomes moving along actin filaments in *Xenopus laevis* melanophore cells obtained in single particle tracking experiments that were reported in previous works [5, 15].

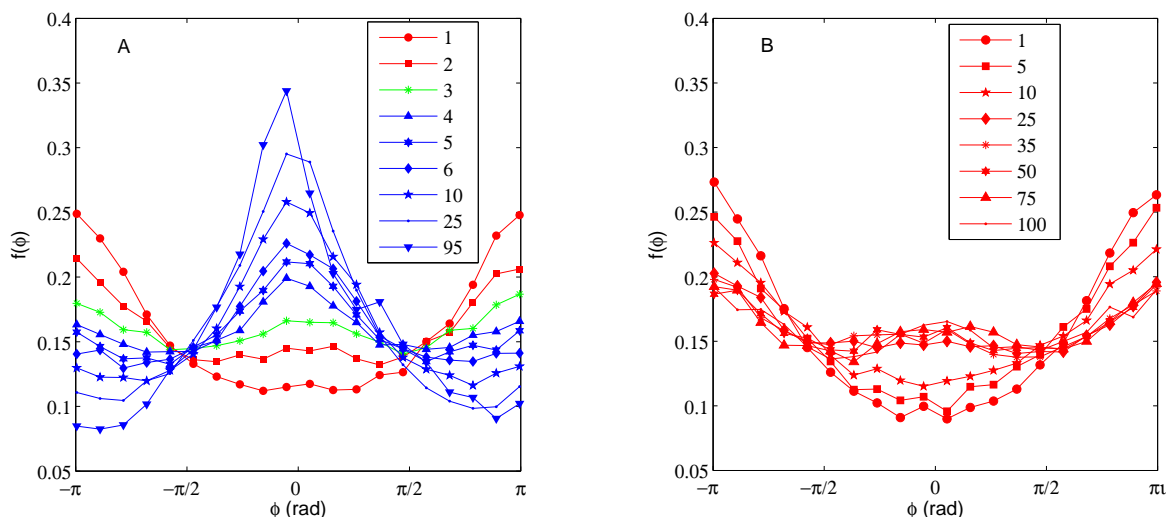


**Figure 1.** Turning angles at different time intervals. (A) Results obtained for WT cells during dispersion ( $n = 33$ ). (B) Results obtained for mutated myosin-V cells ( $n = 15$ ).

Melanosomes are black pigment granules with sizes around 500 nm. The experimental

procedure followed to obtain the trajectories is described in Refs. [5, 15]. Importantly, cells were treated with nocodazole to depolymerize microtubules, so the active transport of melanosomes is only driven by the F-actin dependent motor myosin-V.

The experimental data split into two groups: one set was obtained using wild type cells (WT), while the other set was obtained using mutant cells that have a dominant-negative inhibition of myosin-V driven melanosome transport.

Given a 2D trajectory, we define the turning angle  $\phi(\tau)$  as the internal angle between successive segments of duration  $\tau$ . A Matlab script was used to extract the turning angle from the experimental 2D trajectories. For each  $\tau$ , an angle distribution was found. We present the plots for some of these trajectories in Fig. 1.

The peaks of the turning angles distribution function  $f(\phi)d\phi$  shift from  $\phi = \pm\pi$  to  $\phi = 0$  in WT cells (Fig. 1.A) indicating a transition from an antipersistent to a persistent motion. On the contrary, cells expressing the mutation of myosin-V do not develop this transition (Fig. 1.B).

### 3. Determination of the transition time lag

The transition from antipersistent to persistent behavior occurs near an essentially uniform distribution. To directly measure the transition time lag  $\tau^*$  we quantify the departure of the distributions from a uniform one using:

$$\Delta_+ = \left| \int_0^{\pi/2} f(\phi)d\phi - \int_{\pi/2}^{\pi} f(\phi)d\phi \right| \quad (1)$$

$$\Delta_- = \left| \int_0^{-\pi/2} f(\phi)d\phi - \int_{-\pi/2}^{-\pi} f(\phi)d\phi \right| \quad (2)$$

We define  $\tau^*$ , the time of the transition, as the time lag that minimizes this difference. A similar approach was used in [6]. This method resulted effective since we found a clear minimum for  $\Delta_+$  and  $\Delta_-$  (Fig. 2).

In a previous paper [5] the transition was analyzed using a stochastic model based on the Langevin generalized equation. Within this approach, the dynamics of a melanosome of mass  $m$ , immersed in the intracellular medium and simultaneously driven by molecular motors is described as follows:

$$m\ddot{X}(t) + \int_0^t dt' \gamma(t-t') \dot{X}(t') = \bar{\xi}(t) + \bar{\chi}(t), \quad (3)$$

where  $\gamma(t)$  is the dissipative memory kernel,  $\bar{\xi}(t)$  is an internal noise (related to the subdiffusive passive transport) and  $\bar{\chi}(t)$  is an external noise related to the active transport due to the action of molecular motors. Assuming power-law correlation functions with exponents  $\lambda$  and  $\alpha$ , respectively, for both types of noise, the mean square displacement (MSD) for the long time limit is given by [5]:

$$MSD(\tau) = \frac{4k_B T}{\gamma_0} \left\{ \frac{1}{\Gamma(\lambda+1)} \tau^\lambda + \varepsilon K_{\lambda,\alpha} \tau^{2\lambda-\alpha} \right\} + 2\eta^2, \quad (4)$$

where

$$K_{\lambda,\alpha} = \Gamma(\alpha-2\lambda) \frac{\sin(\pi(\lambda-\alpha)) - \sin(\pi\lambda)}{\pi} \quad (5)$$

is a positive constant, being  $\lambda < 1$  and  $1 < 2\lambda - \alpha < 2$ . The last term in (4) represents the measurement errors in particle location due to SPT or biological activity [16].

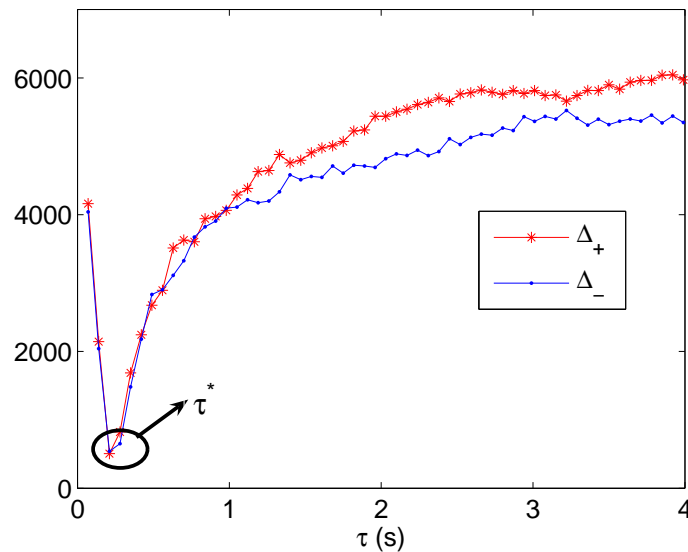


**Figure 2.**  $\Delta_+$  and  $\Delta_-$  as a function of  $\tau$ . The minimum allows to define  $\tau^*$ . The transition occurs for  $\tau^* = 0.21\text{s}$  in the case shown in the figure.

The MSD local slope (in double log scale) is given by:

$$\beta(\tau) = \frac{\frac{\lambda}{\Gamma(\lambda+1)}\tau^\lambda + \varepsilon(2\lambda - \alpha)K_{\lambda,\alpha}\tau^{2\lambda-\alpha}}{\frac{1}{\Gamma(\lambda+1)}\tau^\lambda + \varepsilon K_{\lambda,\alpha}\tau^{2\lambda-\alpha} + \delta}, \quad (6)$$

where  $\delta = \gamma_0 \eta^2 / 2k_B T$ .

For short time lags the dominant term is the subdiffusive one (given by  $\lambda$ ) and for larger time lags the superdiffusive term prevails (given by  $2\lambda - \alpha$ ). So, the transition occurs when  $\beta(\tau^*) = 1$ .

It can be seen in Fig. 3 that the dependence of the asymptotic slope of the MSD (given by  $2\lambda - \alpha$  in the model) with the transition time obtained from the analysis of the turning angle distributions agrees with the prediction of Eq. (6) with  $\beta(\tau^*) = 1$ . Therefore, there is a close correlation between subdiffusion and antipersistence, and superdiffusion and persistent motion in melanosome transport driven by molecular motors.

Moreover, Fig. 3 shows that the transition occurs earlier for trajectories that have larger values of  $2\lambda - \alpha$ . An intuitive explanation of this is the following: assuming a given value of  $\lambda$ , larger  $2\lambda - \alpha$  implies lower values of  $\alpha$ . Let us recall that  $\alpha$  is the exponent of the autocorrelation function of the force exerted by the motors and that can take values between 0 and 1 [5]. While values of  $\alpha \approx 1$  are related with instantaneous pulse forces [3, 17],  $\alpha \approx 0$  represents a constant force that can give rise to a persistent motion, thus the transition from sub- to superdiffusion will occur earlier. In this condition, it is harder for the thermal forces that drive the particle to randomize the direction of motion. As a consequence, the turning angles are smaller leading to a more persistent motion.

#### 4. Summary

In this work we analyze 2D trajectories of motor-driven pigment organelles obtained by SPT in living cells. We measure the turning angle distributions and found a transition from

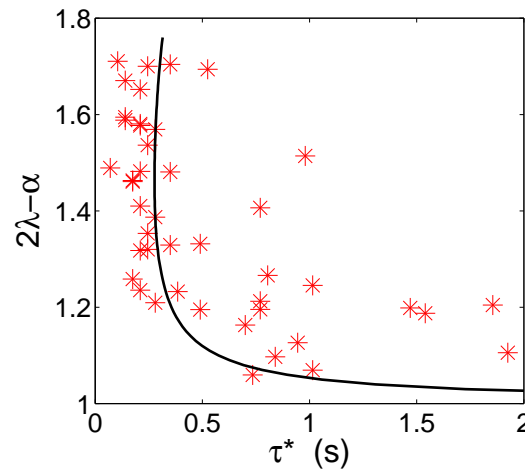


**Figure 3.** Asymptotic slope of  $\log(\text{MSD})$  vs. the critical time (asterisks). The solid line is the dependence of  $2\lambda - \alpha$  with  $\tau^*$ , given by the solution of Eq. (6) with parameter values  $\lambda = 0.9$ ,  $\epsilon = 100$  y  $\delta = 3$ . This parameters agree with those obtained in Ref.[5]

antipersistent to persistent motion. We were able to correlate this transition with the sub-to superdiffusive transition described in a previous work [5].

The approach followed in this paper can be extended to the analysis of other systems to extract information related with the directionality of the trajectories, which cannot be achieved by only studying the MSD.

### Acknowledgments

We acknowledge support from grants PICT 928/06, PICT 31980/05 and PICT 31975/05 from Agencia Nacional de Promoción Científica y Tecnológica, Argentina.

### References

- [1] Levi V, Serpinskaya A S, Gratton E and Gelfand V I 2006 *Biophys. J.* **90** 318
- [2] Tolic-Nørrelykke I M, Munteanu E-L, Thon G, Oddershede L and Berg-Sørensen K 2004 *Phys. Rev. Lett.* **93** 078102
- [3] Wilhelm C 2008 *Phys. Rev. Lett.* **101** 028101
- [4] Gallet F, Arcizet D, Bohec P and Richert A 2009 *Soft Matter* **5** 2947 (2009).
- [5] Bruno L, Levi V, Brunstein M and Despósito M A 2009 *Phys. Rev. E* **80** 011912
- [6] Lenormand G, Chopin J, Bursac P, Fredberg J J and Butler J P 2007 *Biochem. and Biophys. Res. Comm.* **360** 797
- [7] Metzner C, Raupach C, Paranhos Zitterbart D and Fabry B 2007 *Phys. Rev. E* **76** 021925
- [8] Ai B, He Y 2010 *J. Chem. Phys.* **132** 094504
- [9] Magdziarz M and Weron A 2007, *Phys. Rev. E* **75** 056702
- [10] Dybiec B and Gudowska-Nowak E 2009 *Phys. Rev. E* **80** 061122
- [11] Nascimento A A, Roland J T and Gelfand V I 2003 *Annu. Rev. Cell Dev. Biol.* **19** 469
- [12] Tuma M C, Zill A, Le Bot N, Vernos I and Gelfand V I 1998 *J. Cell Biol.* **143** 1547
- [13] Rogers S L, Karcher R L, Roland J T, Minin A A, Steffen W and Gelfand V I 1999 *J. Cell Sci.* **146** 1265
- [14] Nilsson H and Wallin M 1997 *Cell Motil. Cytoskeleton.* **38** 397
- [15] Brunstein M, Bruno L, Despósito M A and Levi V 2009 *Biophys. J.* **97** 1548
- [16] Martin D S, Forstner M B and Käs J A 2002 *Biophys. J.* **83** 2109
- [17] Bursac P, Lenormand G, Fabry B, Oliver M, Weitz D A, Viasnoff V, Butler J P and Fredberg J J 2005 *Nat. Mater.* **4** 557